Iranica Journal of Energy & Environment

Journal Homepage: www.ijee.net

IJEE an official peer review journal of Babol Noshirvani University of Technology, ISSN:2079-2115

An Investigation on the Attack of Dye Species on Freshly Synthesized and Characterized Activated Carbon from Cocoa Pod

P. Chaithra, K. Hemashree, J. Ishwara Bhat*

Department of Chemistry,Mangalore University, Mangalagangothri-574199, India

P A P E R I N F O

Paper history:
Received 23 February 2016
Accepted in revised form 20 April 2016

Keywords:
Activated carbon
Adsorption
Malachite green
Microwave

A B S T R A C T

Activated carbon (AC) was synthesized from raw cocoa pod (RCP) by three activation methods; physical (CPC), chemical (Z CPC, zinc chloride) and microwave activation (MW-CPC). The synthesized AC was characterized using powder X-ray diffraction (XRD), field emission scanning electron microscope (FE-SEM), Fourier transform infrared spectroscopic technique (FT-IR), thermal analysis and differential thermal analysis (TGA-DTA), atomic absorption spectroscopic technique (AAS) and flame photometer instrument. The characterization data reveals that microwave activated carbon having good adsorbent character than physical and chemical activated carbon. Adsorption of malachite green on CPC, Z CPC and MW-CPC were studied at various experimental condition. Freundlich adsorption isotherm model holds good for the adsorption process. The mechanism of adsorption followed the second order kinetics. Thermodynamics of adsorption were studied. The amount of dye adsorbed onto activated carbons varies in the order MW-CPC (29.3632mg/g) > CPC (29.3537mg/g) > Z CPC (27.9905mg/g).

***doi**: 10.5829/idosi.ijee.2016.07.04.05*

INTRODUCTION

Activated charcoal or carbon (AC) is a carbonaceous material having high adsorption capacity due to its amorphous nature, surface porosity, large surface area, surface functional groups and high degree of surface reactivity [1- 4]. Dyes are widely used in industries such as textile, rubber, plastics, printing, cosmetics etc., to color their product [5]. Most of the dyes have been identified as toxic or carcinogenic towards environment. The methods employed to removal of dyes from the solution with the process of adsorption onto activated carbon are adsorption onto activated carbon, photocatalysis, precipitation (coagulation, flocculation and sedimentation), reverse osmosis, incineration, aerobic and anaerobic treatment etc [6,7]. Researchers investigated the adsorption of environmentally harmful synthetic dyes onto activated carbon from agricultural waste products [8-13]. In addition, conversion of lignocellulosic waste to activated carbon is considered in an economical process with significant energy saving.

In the present research work activated charcoals were synthesized using raw cocoa pod (Theobroma Cacao) from three different methods; physical, chemical and microwave activation. The obtained charcoals are CPC, Z CPC and MW-CPC. The powder X-ray diffraction technique was used to characterized the AC samples. FE-SEM was employed to analyze the surface morphology of physical (CPC), chemical (Z CPC) and microwave activated charcoal (MW-CPC) before and after adsorption. FT-IR technique was used to determine the surface functional groups present on raw and activated charcoals. TGA-DTA instrument was used to study the thermal stability and decomposition of RCP and AC. Atomic absorption and Flame photometer were used to analysis of surface elements of physical, chemical and microwave activated cocoa pod charcoal. The present work also investigates on the adsorption capacity of three different AC (CPC, Z CPC and MW-CPC) at various experimental condition. Malachite green oxalate powder a basic dye was selected as an adsorbate for the present adsorption system. As for the literature review the present adsorption system is new since no work has been reported based on the present adsorbte and adsorbent combination. The adsorption data were fitted with Freundlich and Langmuir adsorption isotherm model. The kinetics of

* Corresponding author: J. Ishwara Bhat
E-mail: bhatij@yahoo.com; Phone:9448409998; Fax : (0824) 2287367

Please cite this article as: P. Chaithra, K. Hemashree, J. Ishwara Bhat, 2016. An Investigation on the Attack of Dye Species on Freshly Synthesized and Characterized Activated Carbon from Cocoa pod, Iranica Journal of Energy and Environment 7 (4): 350-358.

adsorption also studied using first order and second order rate equation to know the mechanism of adsorption. Thermodynamic parameters of adsorption were evaluated. A design strategy was considered as energy saving concept in conversion of lignocellulosic wase to activated carbon.

Material and Methods

Adsorbent material

The activated charcoal was synthesized from the raw cocoa pod (RCP) collected from local agricultural field. The raw sample was subjected to three different activation methods namely physical, chemical (zinc chloride) activation in muffle furnace (300 °C, 2h) [14] and microwave activation (80 W, 280 min) in domestic micro oven. Such resulted activated charcoal was crushed in mortar to make it a powder and was sieved in 250 µm pass to get uniform sized activated carbon.

Adsorbate material

The adsorbate material used in the present work is malachite green oxalate purchased from Sisco Research Laboratories (Pvt. Ltd. Mumbay, India). (*M.W*=927.02g/mol, λ_{max}=618nm). The molecular structure of malachite green oxalate is shown in Figure 1.

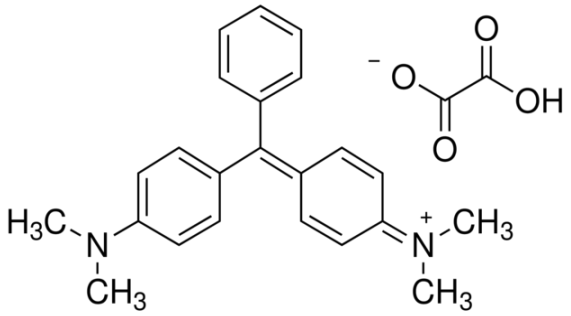

Figure 1. Molecular structure of Malachite green oxalate

Characterization of activated charcoal

Nature of the synthesized activated charcoal (CPC, Z CPC and MW-CPC) was analyzed using powder x-ray diffractometer (RigakuMiniflex 600 diffractometer) using Cu-*Kα* (*λ*=1.5418 Å) operating voltage=40KV and a current of 15mA. The diffraction angle range was 2θ=10° to 55°. The surface image was scanned using Carl Zeiss field emission scanning electron microscope with a magnification 2.50 KX and EHT=5.00kV. Functional groups present on the surface of AC were identified by fourier transform infrared spectroscopic technique (Shimadzu FT-IR Prestige-21, ATR method). The FT-IR spectra were recorded in wavenumber range of 4000-500cm^{-1}. Thermal stability of samples were studied by thermogravimetric analysis (TA) and differential thermal analysis (DTA) using a TA-STD Q600 instrument under dry nitrogen atmosphere at the flow rate of 100mL/min. The samples were heated from 50°C to 700 °C at predetermined rate of 20 °C/min. Solution of activated charcoal [15] was subjected to elemental analysis using AAS (GBC 932 Plus Atomic Absorption Spectrometer) and Flame photometer (Systronics Flame photometer 130) with Na and K filters.

Adsorption studies

The adsorption of malachite green in aqueous medium onto synthesized activated carbon (CPC, Z CPC and MW-CPC) was studied at different experimental condition. The activated carbon (0.1g) and malachite green solution (40mg/L, 50mL) were taken in a reagent bottle and kept on a magnetic stirrer for 1h. The initial and final concentration of malachite green solutions were determined by measuring absorbance at 618 nm using UV-visible spectrophotometer. The amount of dye adsorbed per unit mass of activated carbon were calculated as follows [16]:

$$q = \frac{(C_0 - C_e)V}{W} \quad (1)$$

where C_0 is the initial concentration of dye (mg/L); C_e is the concentration of dye in the solution after adsorption (mg/L); V is the volume of the solution (mL); and W is the weight of activated carbon (g).

RESULTS AND DISCUSSION

Powder XRD analysis

The X-ray diffraction pattern of physical, chemical and microwave activated cocoa pod charcoal were shown in Figure 2.

It is clear from the Figure 2, that physical and microwave activated carbons appeared to be more amorphous than chemical activated charcoal. Sharp intensed three peaks were recorded in XRD pattern of Z CPC indicates the presence of crystallites in the powder of AC, which were reflected from the calculated (111) and (200) planes. The diffraction peaks appeared at 32°, 34.7°, 36.5°, 47.8° indicates the presence of ZnO [17-19]. Elemental analysis data proposed the presence of maximum concentration of zinc on Z CPC (Table 4.). The likely crystalline (sharp andintensed) peak regions and amorphous (weak and small) peak regions of CPC, Z CPC and MW-CPC are shown in Table 1.

The crystallite size of AC's were calculated from Scherer's formula [20]. Structural deformation was evaluated using calculated values of defect density and lattice strain [21]. Crystallinity index (*CrI*) of all the three

TABLE 1. The diffraction angle θ (degree), Intensity, Lattice spacing d (A^0), N, reflection plane (hkl) and cell parameter a (A^0) values are calculated for the diffraction peaks of CPC, Z CPC and MW-CPC.

Adsorbents	2θ(degree)	Intensity	d (A^0)	N	hkl	a ($d\sqrt{N}$) (A^0)
CPC	19.19	285.37	4.6249	1	(100)	4.5757
	22.1	324	4.0221	1	(100)	
	24.5	391	3.6332	2	(110)	
	25.9	386	3.439	2	(110)	
	30.3	280	2.949	2	(110)	
	33.5	190	2.674	3	(111)	
Z CPC	18.9	275	4.6952	1	(100)	4.6949
	23.6	362	3.7697	2	(110)	
	32	533	2.7967	3	(111)	
	34.7	434	2.5851	3	(111)	
	36.5	765	2.4616	4	(200)	
	42.2	165	2.1414	5	(210)	
	47.8	273	1.9027	4	(200)	
MW CPC	16	237	5.53911	1	(100)	5.4921
	17.28	255	5.1316	1	(100)	
	22.29	357.37	3.9882	2	(110)	
	23.16	307	3.8403	2	(110)	
	27.53	282.32	3.2398	3	(111)	
	35.86	173	2.5041	5	(210)	

TABLE 2. Cell volume (v), Crystallite size (D), defect density (δ), lattice strain (η) and crystallinity index (CrI) values are shown.

Adsorbents	v(A^0)^3	D(A^0)	δ (A^0)$^{-2}$	η	CrI
CPC	95.80	0.0534	350.68	30.56	27.01
Z CPC	103.49	0.0483	428.65	22.89	64.05
MW CPC	165.66	0.0540	342.93	33.18	21.92

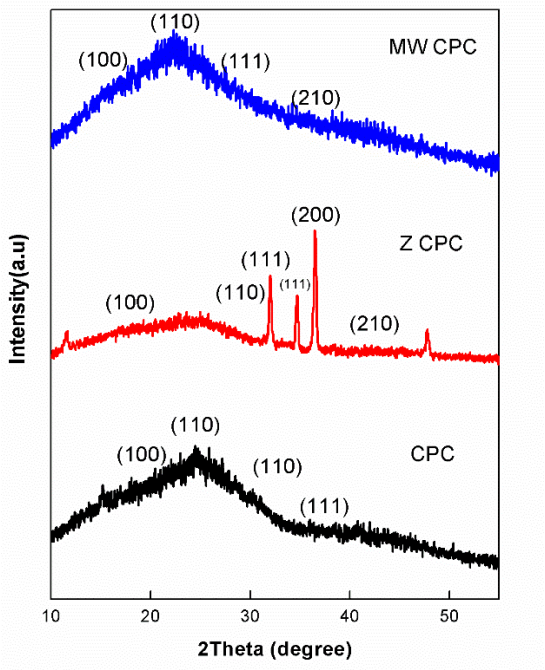

Figure 2. XRD pattern of CPC, Z CPC and MW- CPC

different carbons were calculated [19]. The cell volume, crystallite size and lattice strain of AC's varies in the order of MW-CPC > CPC > Z CPC. The defect density was found more in Z CPC which may be due to the possibly chemical interaction between zinc ion and carbon [14]. The crystallinity index (CrI) gives an idea on the total crystallinity of sample. CrI was calculated and presented in Table 2.

FE-SEM analysis

Surface of AC's (CPC, Z CPC and MW-CPC) was scanned by FE-SEM and scanned images were shown in Figure 3 (a, b and c). Pores of different size were identified on the surface of the three carbons. Defects on the AC surface was observed. This defects decides the adsorption capacity of that AC. From the image it may also be concluded that the surface porosity varies in the order MW-CPC > CPC > Z CPC. The SEM image of dye adsorbed CPC, Z CPC and MW-CPC are shown in Figure 3 (d, e and f). On adsorption of the dye the pores were found to be filled or blocked.

FT-IR Analysis

The FT-IR spectra of raw cocoa pod (RCP) and activated carbon samples (CPC, Z CPC and MW-CPC) are shown in Figure 4.

The FT-IR spectra of AC appears to be fully different from the raw cocoa pod (Figure 4.), shows a broad O-H

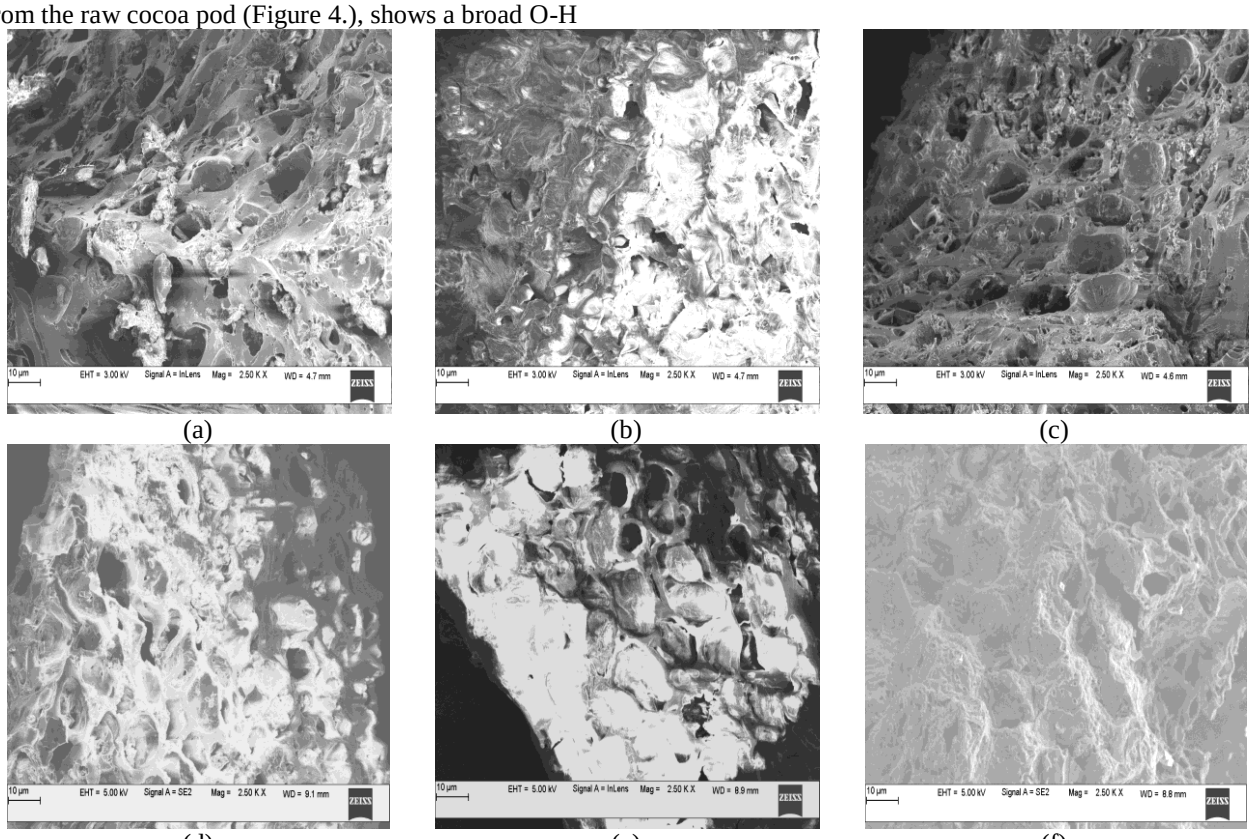

Figure 3. SEM image of (a) CPC, (b) Z CPC, (c) MW-CPC, (d) dye adsorbed CPC, (e) dye adsorbed Z CPC, (f) dye adsorbed MW-CPC.

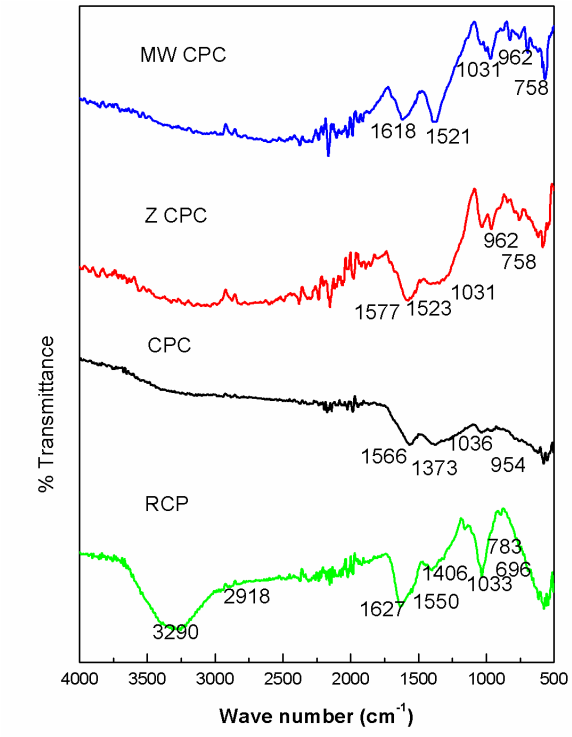

Figure 4. FT-IR Spectra of RCP, CPC, Z CPC and MW-CPC.

peak at 3290cm^{-1}, C-H stretching vibrations at 2918cm^{-1}. These two peaks were not observed in synthesized activated carbons. This indicates the structural changes from raw sample to activated samples has occurred due to the decomposition of some of the functional groups present in the raw material during the activation process. The carbonyl (C=O) stretching was observed in all the synthesized carbon but not at the same wave number. This shows that there is change in surface of AC prepared from three different activation methods. Ether C-O-C stretching was observed at the range from 1036 to 1031cm^{-1} in raw and activated carbons. The stretching frequency corresponds to at 1406 and 1373 cm^{-1} is due to C-N vibration. The IR peaks at 1000-750cm^{-1} corresponds to C-H out of plane bending in all the raw and AC samples. Characteristic infrared absorptions of functional groups recorded in CPC, Z CPC and MW-CPC shown in Table 3. The TGA-DTA analysis of raw and AC's are shown in Figure 5(a-d). were supports this observation that is the percentage decomposition from raw cocoa pod was found to be maximum than AC's.

Thus FT-IR technique was useful in differentiating the raw and activated carbons.

TGA-DTA Analysis

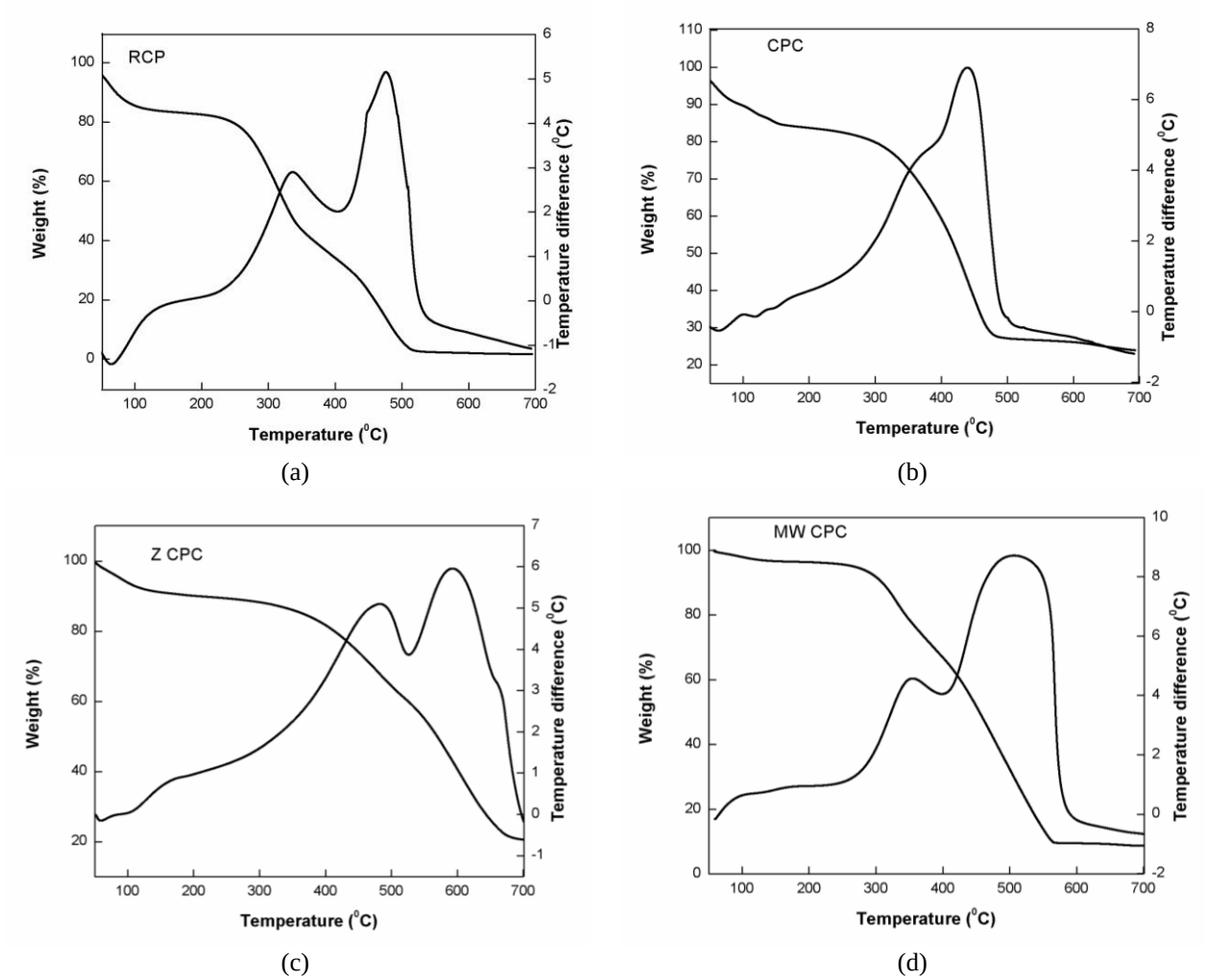

Figure 5. TGA-DTA Pattern of **(**a) RCP, (b) CPC, (c) Z CPC, (d) MW-CPC.

TGA-DTA pattern of RCP, CPC, Z CPC and MW-CPC are shown in Figure 5 (a, b, c and d).

Thermogravimetric analysis (TGA) enabled us to know the thermal stability and also the steps involved in decomposition of the sample. In thermogravimetry change in mass of the sample is recorded as a function of temperature. Thermal decomposition of RCP, CPC, Z CPC and MW-CPC (see Figure 5.) showed the presence of three specific degradation steps. These three steps indicates respectively the evaporation of moisture (step 1: 200 ◦C) a sharp decomposition likely presence of hemi cellulose and cellulose was observed (step 2: 200 to 400 ◦C) and also the decomposition of carbonyl groups present in lignin (step 3: 400 to 500 ◦C). Differential thermogram were plotted for the difference in temperature between sample and inert reference against overall furnace temperature. The decomposition temperature of samples varies in the order Z CPC > MW-CPC > RCP > CPC. The temperature decomposition weight loss varies in the order of RCP > CPC > Z CPC > MW-CPC at 200◦C. This clearly indicates that raw cocoa pod has maximum moisture content on the surface. This supports the broad O-H peak obtained for under IR spectra (see Figure 4.).

Surface elemental analysis

The elements present in the activated charcoal were found by AAS and flame photometer. The resulted values are shown in Table 4.

Activated charcoals (CPC, Z CPC and MW-CPC) are of plant origin. The elements such as Cr, Fe, Ni, Cu, Zn, Pb, Na, K etc., appeared here might be due to the nutrient absorbed by the plant during its grown. The maximum Na^+ concentration was identified in the case of CPC and MW-CPC. Similar observation was also

made by Turoti and Bello [15]. Zinc was the major element in Z CPC may be due to retention of Zn^{2+} ion on the surface.

Adsorption studies

TABLE 3. Characteristic infrared absorptions of functional groups recorded in CPC, Z CPC and MW-CPC

Functional group	Intensity range (cm^{-1})
A. Hydrocarbon	
1. C-H out of plane bending	1000-750
2. C=C stretching, Aromatic alkene	1600-1500
B. Carbonyl groups(C=O)	
1. Carboxylic acids carboxylate anion stretching	1618-1521
2. Ether, C-O-C stretching	1036-1031
C. Miscellaneous groups	
Amines , C-N vibration Primary, Secondary and tertiary	1373

Adsorption isotherm

Adsorption experiment was carried out at varying concentration of dye (20-60 mg/L). Experimental condition : Weight of AC, *W*=0.1g, volume of malachite green solution *V*=50mL, agitation time *t*=60min. In the present study adsorption data were fitted with Freundlich and Langmuir adsorption isotherm.

The Freundlich adsorption isotherm equation is given by [23]

$$\log q_e = \log k_f + \frac{1}{n}\log C_e \qquad (2)$$

where k_f and n are the Freundlich constants for a given adsorbate and adsorbent at a particular temperature. Which are helpful in finding the feasibility of adsorption process and there by comparing the adsorption efficiency of adsorbent. A linear plot of *log* q_e versus *log* C_e was obtained and shown in Figure 6a. slope and intercept gives n and k_f values shown in Table 5. Langmuir adsorption isotherm equation is stated as follows [24]

$$\frac{C_e}{q_e} = \frac{C_e}{q_m} + \frac{1}{q_m b} \qquad (3)$$

where *Ce* is concentration of dye adsorbed at equilibrium, q_e is the amount of dye adsorbed at equilibrium, q_m and *b* are Langmuir constants which indicates the monolayer adsorption capacity and the adsorption intensity of adsorbent. Linear plot observed for the plot of Ce/q_e versus *Ce* is sown in Figure 6b. From the slope and intercept of the above linear plot, value of q_m and *b* can be calculated. Equilibrium parameter R_L was calculated [24] and shown in Table 5.

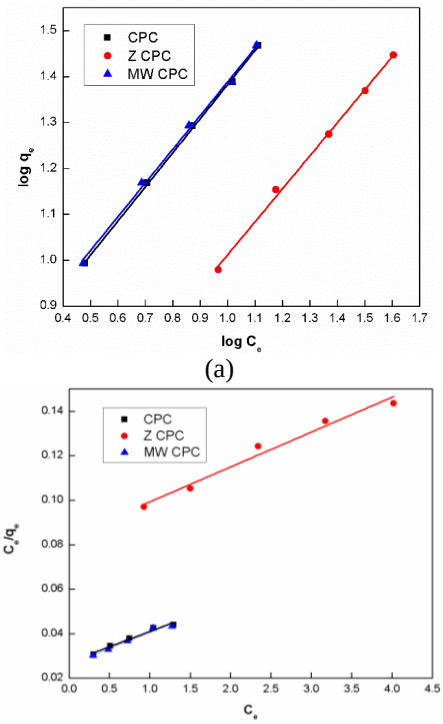

Figure 6. (a) Freundlich adsorption isotherm plot, (b) Langmuir adsorption isotherm plot of adsorption of dye on (▪) CPC, (●) Z CPC & (▲) MW-CPC.

The value of Freundlich constant n is more than 1 in all the carbons hence Freundlich adsorption isotherm model suits for the present adsorption process [23]. The Langmuir equilibrium parameter R_L value lies in the range 0 and 1 which indicates favorability of adsorption. The R^2 value for Langmuir plot is lower than that of Freundlich adsorption isotherm plot. Therefore Freundlich adsorption isotherm model is best fits for the adsorption of dye on the surface of CPC, Z CPC and MW-CPC.

Kinetics of adsorption

The kinetics study of adsorption helps to know the mechanism of the adsorption process and allows one to calculate the maximum rate at which surface sites can be occupied by dye molecules. The first order and second order kinetic models were adopted to determine the rate constant of adsorption process. The first order rate equation is given as follows [25]:

TABLE 4. Concentration (ppm) of elements present in the activated charcoal samples.

Adsorbents	Cr	Fe	Ni	Cu	Zn	Pb	Na	K

CPC	4.00	0.50	0.42	0.25	5.25	1.25	10.00	0.42
Z CPC	1.00	0.35	0.34	0.50	2000	1.25	1.00	0.34
MW CPC	1.25	0.25	0.35	0.50	3.25	1.25	8.00	0.35

TABLE 5. Freundlich and Langmuir adsorption isotherm constants for adsorption of malachite green onto CPC, Z CPC and MW-CPC.

Adsorbents	n	k_f	R^2	b	R_L	R^2
CPC	1.34	4.36	0.999	0.50	0.054	0.969
Z CPC	1.39	1.96	0.996	0.19	0.129	0.970
MW CPC	1.36	4.51	0.996	0.55	0.049	0.969

$$\log(q_e - q_t) = \log q_e - \frac{k_1 t}{2.303} \quad (4)$$

where q_e is the amount of dye adsorbed at equilibrium and q_t is the amount of dye adsorbed at time t; k_1 is the first order rate constant. A plot of *log* $(q_e - q_t)$ versus t was found to be non linear. Hence first order kinetics not holds good for the present adsorption process.

Second-order kinetics equation is as shown below [26]

$$\frac{t}{q_t} = \frac{1}{k_2 q_e^{\,2}} + \frac{t}{q_e} \quad (5)$$

where k_2 is the second-order rate constant and it was calculated from the slope of linear plot t/q_t versus t as shown in Figure 7. and Table 6.

Second order rate constant for the adsorption of dye on AC's varies in the order

MW-CPC > CPC > Z CPC. The rate depends on amount of activated carbon (adsorption site) and concentration of dye. Hence mechanism of adsorption may be summariesed as follows [2]

$$A_d + S_a = A_dS_a \qquad \Delta H^{\ddagger} < 0 \quad (6)$$

where A_d is the adsorbate or dye molecule and S_a is the adsororption site on adsorbent or activated carbon. The change in enthalpy of adsorption ($\Delta H^{\ddagger}$) is less than zero (Table 7); it indicates that adsorption of dye molecules onto activated carbons are exothermic process. The FT-IR spectra of CPC, Z CPC and MW-CPC (Figure 4) reveals that the presence of carboxilate anion (COO^-) on the surface of AC. Therefore mechanism of adsorption due to electrostatic interaction between the carboxylate anion of AC surface and the positively charged dye cation in solution. Also the experimental q_e value correlates with the graphical q_e value. Hence the second order kinetics fits well for the present adsorption process.

Thermodynamics of adsorption

Thermodynamics of the present adsorption process was studied at four different temperatures (20, 30, 35 and 50 °C). Thermodynamic parameters energy of activation (E_a), change in enthalpy ($\Delta H^{\ddagger}$), entropy ($\Delta S^{\ddagger}$) and free energy ($\Delta G^{\ddagger}$) were determined using the following equations [27]

$$\log k = \log A - \frac{E_a}{2.303RT} \quad (7)$$

where k is concentration of dye after adsorption (C_e), E_a is the activation energy, A is the Arrhenius parameter, R is gas constant and T is temperature (K). The values of E_a is calculated from the slope of linear plot of *log k* versus *1/T*, (Figure 8a.). The change in enthalpy, entropy and free energy were calculated using absolute theory of rate expression as follows

$$\log\left(\frac{k}{T}\right) = \log\left(\frac{k_B}{h}\right) + \frac{\Delta S^{\ddagger}}{2.303R} - \frac{\Delta H^{\ddagger}}{2.303RT} \quad (8)$$

where k_B is the Boltzmann constant, h is plank's constant. The change in enthalpy ($\Delta H^{\ddagger}$) and change in entropy ($\Delta S^{\ddagger}$) was calculated from the slope and intercepts of linear plot of log (k/T) versus *1/T* as shown in Figure 8b. Change in free energy ($\Delta G^{\ddagger}$) can be calculated using following equation,

$$\Delta G^{\ddagger} = \Delta H^{\ddagger} - T\Delta S^{\ddagger} \quad (9)$$

TABLE 6. Second-order kinetic parameters of the adsorption of dye on CPC, Z CPC and MW-CPC.

Adsorbents	k_2 (g/mg/min)	q_e (mg/g)	R^2
CPC	0.243	19.960	0.999
Z CPC	0.017	17.730	0.997
MW CPC	0.360	19.920	1.00

TABLE 7. Thermodynamic parameters for the adsorption of malachite green onto (▪) CPC, (●) Z CPC and (▲) MW-CPC.

Adsorbents	E_a (kJ/mol)	$\Delta H^{\ddagger}$ (kJ/mol)	$\Delta S^{\ddagger}$ (J/mol/K)	$\Delta G^{\ddagger}$ (kJ/mol)	K_{ads} (kJ/mol)

CPC	-17.704	-20.264	-223.33	48.141	0.981
Z CPC	-2.635	-5.195	-145.165	39.283	0.984
MW CPC	-27.885	-30.444	-259.461	49.001	0.980

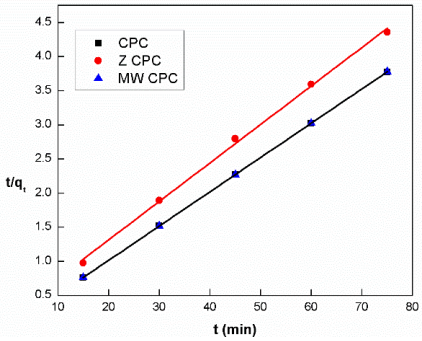

Figure 7. Second order kinetic plot of the adsorption of dye on (▪) CPC, (●) Z CPC and (▲) MW-CPC

From the value of ($\Delta G^{\ddagger}$) adsorption constant K_{ads} can be calculated from the equation,

$$\Delta G^{\ddagger} = -RT \ln K_{ads} \qquad (10)$$

From the Table 7, the activation energy (E_a) was found to be negative for all the three activated carbons. From the experimental data it is clear that as temperature increases the rate of adsorption increases and the dye concentration on the left over solution decreases. Hence activation energy was found to be negative. The change in enthalpy of adsorption $\Delta H^{\ddagger}$ values of adsorption process appears to be negative for CPC, Z CPC and MW-CPC, indicating the exothermic nature of the process. The $\Delta S^{\ddagger}$ value in the present process was found to be negative as required for an adsorption process. On adsorption the degree of randomness or degree of freedom of molecules gets decreased and the particles become stable on the surface upon adsorption. The change in free energy $\Delta G^{\ddagger}$ was positive. Values of K_{ads} were calculated and shown in Table 7.

CONCLUSION

The activated carbons were synthesized from raw cocoa pod by physical, chemical and microwave activation methods. The synthesized carbons were characterized using powder XRD, FE-SEM, FT-IR, TGA-DTA, AAS and flame photometer instruments. The characterization result reveals that microwave activated carbon has better adsorbent character than physical or chemical activated cocoa pod charcoal. The adsorption of malachite green onto activate carbons (CPC, Z CPC and MW-CPC) were studied and compared. The Freundlich adsorption isotherm was found to best fit for the present study. The present adsorption process followed the second order kinetics. Evaluation of thermodynamic parameter ($\Delta H^{\ddagger}$, $\Delta S^{\ddagger}$ and $\Delta G^{\ddagger}$) showed the exothermic nature of adsorption of malachitegreen on CPC, Z CPC and MW-CPC. MW CPC has maximum dye adsorption capacity compared either with CPC or Z CPC.

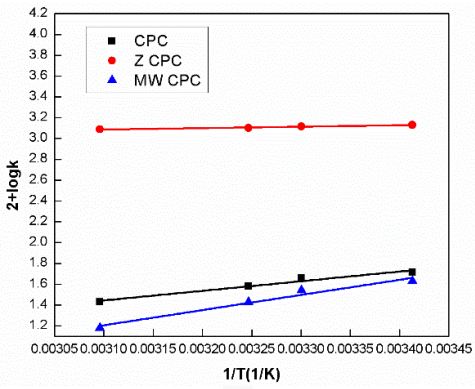

(a)

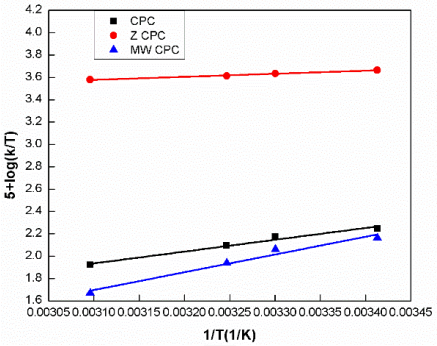

(b)

Figure 8. Plot of (a) 2+*log k* Vs *1/T*, for the adsorption of malachite green onto (▪) CPC, (●) Z CPC & (▲) MW-CPC (b) 5+log(*k/T*) Vs *1/T*

Acknowledgements

The authors are thankful to the Co-ordinator, DST-FIST Program, USIC and DST-PURSE, Mangalore University for providing instrumental facilities to carry out the present research work. The authors are also thankful to UGC-SAP, Delhi for financial assistance to carry out the present research work.

REFERENCES

1. A.W. Adamson, 1982. Physical Chemistry of Surfaces, John Wiley and Sons.
2. A. R. Alberty and J.R. Silbey, 1995. Physical Chemisty, John Wiley and Sons.

3. M.S. Shafeeyan, W.M.A.W. Daud, A. Houshmand and A. Shamiri, 2010. A review on surface modification of activated carbon for carbon dioxide adsorption. Journal of Analytical and Applied Pyrolysis. 89: 143-151.
4. D. Das, D.P. Samal and B.C. Meikap, 2015. Preparation of Activated Carbon from Green Coconut Shell and its Characterization, Journal of Chemical Engineering and Process Technology, 6(5): 1-7.
5. R. Gandhimathi, S.T. Ramesh, V. Sindhu and P.V. Nidheesh, 2014. Removal characteristics of basic dyes from aqueous solutions by fly ash in single and tertiary systems, Joural of Scientific and Industrial Research, 73(4): 267-272.
6. T. Ibrahim, B.L. Moctar, K. Tomkouani, D.B. Gbandi, D.K. Victor and N. Phinthe, 2014. Kinetics of the Adsorption of Anionic and Cationic Dyes in Aqueous Solution by Low-Cost Activated Carbons Prepared from Sea Cake and Cotton Cake, American Chemical Science Journal, 4(1): 38-57.
7. V.K. Gupta, R. Jain, A. Mittal, T. A. Saleh, A. Nayak, S. Agarwal and S. Sikarwar, 2012. Photo-catalytic degradation of toxic dye amaranth on TiO2/UV in aqueous suspensions, Materials Science and Engineering C. 32(1): 12-17.
8. S. Hashemian and J. Shayegan, 2014. A comparative Study of Cellulose Agricultural Wastes (Almond Shell, Pistachio Shell, Walnut Shell, Tea waste and Orange Peel) for Adsorption of Violet B dye from Aqueous Solutions, Oriental Journal of Chemistry. 30(4): 2091-2098.
9. S.T. Ong, P.S. Keng, S.L. Lee and Y.T. Hung, 2014. Low Cost Adsorbents for Sustainable Dye Containing-Wastewater Treatment, Asian Journal of Chemistry, 26(7): 1873-1881.
10. O.S. Bello, M.A. Ahmad and T.T. Siang, 2011. Utilization of Cocoa pod Husk for the Removal of Remaol Black B Reactive Dye from Aqueous Solutions: Kinetic, Equilibrium and Thermodynamic studies, Trends in Applied Sciences Research, 6(8): 794-812.
11. I.R. Ilaboya, E.O. Oti, G.O. Ekoh and L.O. Umukor, 2013. Performance of Activated Carbon from Cassava Peels for the Treatment of Effluent Wastewate. Iranica Journal of Energy & Environment 4 (4): 361-375.
12. Y.S. Mohammad, E.M. Shaibu-Imodagbe, S.B. Igboro, A. Giwa and C.A. Okuofu, 2014. Adsorption of Phenol from Refinery Wastewater Using Rice Husk Activated Carbon. Iranica Journal of Energy and Environment, 5 (4): 393-399.
13. Y.S. Mohammad, E.M. Shaibu-Imodagbe, S.B. Igboro, A. Giwa, C.A. Okuofu, 2015. Effect of Phosphoric Acid Modification on Characteristics of Rice Husk Activated Carbon. Iranica Journal of Energy and Environment, 6 (1):20-25.
14. K. Ramakrishnan and C. Namasivayam, 2011. Zinc chloride activated Jatropha husk carbon for removal of phenol from water by adsorption: Equilibrium and kinetic studies, Toxicological & Environmental Chemistry, 93(6): 1111-1122.
15. M. Turoti, E. Bello, Cypermethrin Adsorption unto Sodium Chloride-Activated Cacao Theobroma (Cocoa) pod Using Digital GC, World Ru. Obs. 5 (2013) 64-73.
16. P.D. Pathak and S.A. Mandavgane, 2015. Preparation and characterization of raw and carbon from banana peel by microwave activation : Application in citric acid adsorption, 3: 2435-2447.
17. S. Talam, S.R. Karumuri and N. Gunnam, 2012. Synthesis, Characterization, and Spectroscopic properties of ZnO Nanoparticles, ISRN Nanotechnology. 2012(2012): 1-6.
18. Z.M. Khoshhesab, M.Sarfaraz and M.A. Asadabad, 2011. Preparation pf ZnO nano structures by chemical precipitation method, Synthesis and Reactivity in Inorganic, Metal-organic and Nano-metal Chemistry, 41(7): 814-819.
19. J. Zhou, F. Zhao, Y. Wang, Y. Zhang and L. Yang, 2007. Size-controlled synthesis of ZnO nanoparticles and their photoluminescence properties, Journal of Lumiescence, 122(1): 195-197.
20. M.M.B. Abbad, A.A.H. Kadhum, A.B. Mohamad, M.S. Takriff and K.Sopian, 2012. Synthesis and Catalytic Activity of TiO2 Nanoparticles for Photochemical Oxidation of Concentrated Chlorophenols under Direct Solar Radiation, Inernational Journal of Electrochemical Science, 7(6): 4871 – 4888.
21. Z.R. Khan, M.S. Khan, M. Zulfequar and M.S. Khan, 2011. Optical and Structural Properties of ZnO Thin Films Fabricated by Sol-Gel Method, Materials Sciences and Applications, 2(5); 340-345.
22. L.P. Xiao, Z.J. Sun, Z.J. Shi, FengXu and R.C. Sun, 2011. Impact of hot compressed water pretreatment on the structural changes of woody biomass for bioethanol production, BioResources, 6(2): 1576-1598.
23. M.A. Ahmad, N. Ahmad and O.S. Bello, 2015. Adsorption Kinetic Studies for the Removal of Synthetic Dye Using Durian Seed Activated carbon, Journal of Dispersion Science and Technology. 36(5): 670-684.
24. D. Sun, Z. Zhang, M. Wang and Y. Wu, 2013. Adsorption of Reactive Dyes on Activated Carbon Developed from Enteromorpha prolifera, American Journal of Analytical Chemistry, 4(7A): 17-26.
25. S.K. Deokar, S.A. Mandavgane and B.D. Kulkarni, 2016. Behaviour of biomass multicomponent ashes as adsorbents, Current Science, 110(2): 180-186.
26. S.M. Yakout and M.M.S. Ali, 2011. Sorption of cationic dyes onto activated carbon derived from agro-residues, Journal of Atomic and Molecular Sciences, 2(2): 117-128.
27. M.H. Karaoglu, S. Zor and M. Ugurlu, 2010. Biosorption of Cr(III) from solutions using vineyard pruning pruning waste, Chemical Engineering Journal, 159(13): 98-106.

.

Persian Abstract

DOI: 10.5829/idosi.ijee.2016.07.04.05

چکیده

با استفاده از روش های فیزیکی، شیمیایی و کمک مایکروویو غلاف کاکائو به کربن فعال تبدیل شد. کربن فعال تولید شده با استفاده از آنالیز XRD، FE-SEM ، FT-IR، TGA، AAS و PFI مورد ارزیابی قرار گرفت. نتایج نشان از آن دارد که کربن فعال تولید شده با استفاده از روش مایکروویو مشخصات جذب بهتری از سایر موارد دارد. در این مطالعه جذب رنگ مالاشیت سبز در شرایط مختلف مورد ارزیابی قرار گرفت. همچنین ترمودینامیک جذب برای این ماده بر روی جاذب های تولیدی مورد مطالعه قرار گرفت.